

Smart, Stretchable Supercapacitors

Xuli Chen, Huijuan Lin, Peining Chen, Guozhen Guan, Jue Deng, and Huisheng Peng*

Electrochemical capacitors have been widely studied for energy storage due to their high specific capacitances and power densities.^[1–12] Besides the enthusiastic devotion to enhance the electrochemical performance, increasing interests are attracted to integrate more functions to extend the application range. For instance, electrochemical capacitors were made flexible and stretchable to meet the development in the portable and wearable electronics.^[13] Meanwhile, it will be very useful to make electrochemical capacitors smart, e.g., sensing changes in the level of stored energy and being able to respond to the changes in a predictable and noticeable manner. A difficulty we have to confront in our daily life is to quickly determine whether the energy has been consumed out before a device stops working. Therefore, these dynamic communications bring a lot of convenience with high efficiency to promote widespread applications of electrochemical capacitors, and may represent a promising breakthrough in science and technology.

Conducting polymers have been widely studied as a family of smart materials as they exhibit obvious changes in colors in response to various environmental stimuli including temperature, pH, ion, solvent, and ligand interaction.^[14] Recently, it was found that, by introduction of aligned carbon nanotubes (CNTs), the resulting conducting polymer composite films and fibers demonstrated chromatic transitions upon pass of electric currents with a high reversibility, and the colors could be accurately controlled by varying the values of passed currents or used voltages.^[15] This colorimetric change can be easily perceived by the naked eyes, making them ideal candidates for sensing applications. Although the conjugated polymers are widely explored for smart materials, it remains unavailable to realize smart energy devices such as supercapacitors.

In this Communication, we have developed smart electrochemical capacitors by depositing polyaniline (PANI) onto aligned CNT sheet electrodes. The capacitors rapidly and reversibly change colors among yellow, green and blue, which can be immediately observed by our naked eyes, to directly indicate their working states. A specific capacitance of 308.4 F/g has been achieved. Due to the continuous, aligned structure in the composite electrode, the smart capacitors are also stretchable and flexible with a high stability, and the specific capacitances have been well maintained after stretching up to 100% for 200 cycles or bending for 1000 cycles.

The fabrication of the stretchable supercapacitor is schematically shown in **Figures 1** and S1. A stretchable polydimethylsiloxane (PDMS) film that has been prepared by a spin-coating process is firstly pre-stretched. A thin layer of aligned CNT sheet is paved onto the stretched PDMS substrate to make a stretchable, electrically conducting film, followed by deposition of PANI through electropolymerization of the monomer, i.e., aniline. The stretched electrode is then released and coated with a gel electrolyte. The stretchable supercapacitor is finally fabricated by assembling the two stretchable electrodes together.

Figure 2 shows scanning electronic microscopy (SEM) images of a typical stretchable electrode. The aligned CNT sheets were dry-drawn from spinnable CNT arrays that had been synthesized by chemical vapor deposition.^[16,17] The aligned CNT sheet typically with a thickness of ~20 nm could be stably attached onto the stretched PDMS film, and no CNTs had been obviously peeled off from the substrate traced by the SEM even after bending for many cycles (**Figure 2a**). The resulting thin CNT sheets were transparent with optical transmittances over 90%, and they exhibited high electrical conductivities on level of 10^2 – 10^3 S/cm.^[17,18] As designed, the paved CNTs were aligned to enable high electrical conductivities that were necessary for the high performance of the resulting supercapacitor (**Figure 2b**). As expected, PANI had been well coated on the CNT sheet to produce high-quality composite films where the CNTs retained the aligned structure even at a PANI weight percentage of 70% (**Figures 2c** and **2d**). After release to the non-stretched state, the CNTs remained aligned in the composite electrode, and a crumbled structure was formed to enable a high stretchability (**Figures 2e** and **2f**).^[19]

The resulting supercapacitor exhibited a high electrochemical performance. **Figure 3a** has compared Galvanostatic charge-discharge profiles of supercapacitors based on different PANI weight percentages at 1 A/g, and the maximal specific capacitance appears at 70%. To further explore the influence of PANI weight percentage on the specific capacitance, Galvanostatic charge-discharge processes were also carried out at the increasing current densities from 1 to 8 A/g. As shown in **Figure 3b**, the specific capacitances were gradually enhanced from 153.4 to 308.4 F/g with the increasing PANI weight percentage due to the improved pseudo-capacitance from the PANI. With the increasing current densities from 1 to 8 A/g, the capacitances had been maintained by 81.7%, 79.8% and 73.9% at PANI weight percentages of 20%, 50% and 70%, respectively, while the specific capacitance retention dropped to 25.6% at a higher weight percentage of 90% although a high capacitance of 335.8 F/g was achieved (**Figure S2**). This phenomenon may be explained by the decreasing conductivities with the increasing PANI weight percentage (**Figure S3**).^[20] Considering the combined excellent property in the specific capacitance and rate capability, the PANI weight percentage of 70% had been mainly investigated in the following discussion.

X. Chen, H. Lin, P. Chen, G. Guan,
J. Deng, Prof. H. Peng
State Key Laboratory of Molecular
Engineering of Polymers
Department of Macromolecular Science
and Laboratory of Advanced Materials
Fudan University
Shanghai 200438, China
E-mail: penghs@fudan.edu.cn



DOI: 10.1002/adma.201400842

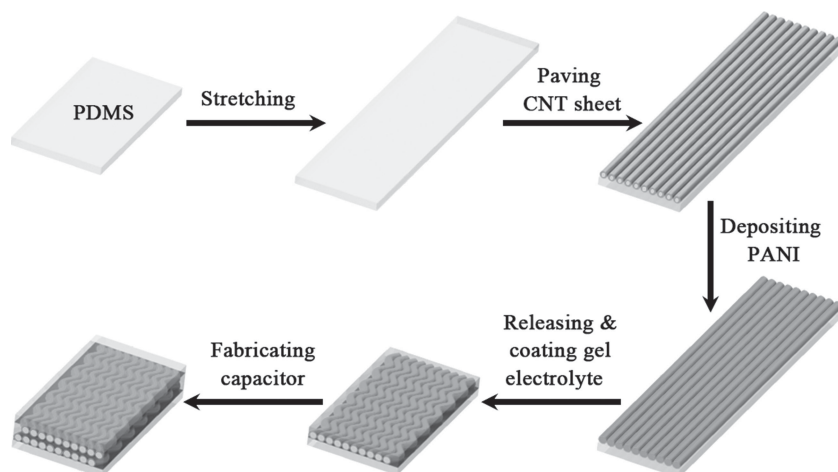


Figure 1. Schematic illustration to the fabrication of the smart, stretchable and flexible supercapacitor.

Note that PANI was widely studied to form composites with carbon nanomaterials such as graphene besides CNT for supercapacitors in both two-electrode and three-electrode systems,^[21–27] and the specific capacitances were ranged from 200 to 500 F/g in two-electrode systems, so the smart supercapacitor was comparable with the previous reports.

The composite film electrodes had been also compared with increasing thicknesses of aligned CNT sheets from 20 to 100 nm under the same condition (Figure S4), and the specific capacitance was increased with the increasing thickness due to the decreasing resistance along the aligned direction. However, as expected, the optical transmittance was decreased with the increasing thickness of CNT sheet (Figure S5). Therefore, the CNT sheet with the thickness of 20 nm was mainly studied in this work. Figure 3c shows the cyclic voltammograms with the expected PANI redox peaks for a pseudo-capacitance. In addition, the redox peaks were maintained with the increasing scan rate from 10 to 50 mV/s, indicating a rapid redox reaction of PANI. Figure 3d further shows Galvanostatic charge-discharge curves at increasing current densities from 1 to 8 A/g. The symmetric curves can be well maintained, which further verifies the good rate capability. Figure 3e shows the long life stability of the supercapacitor. The specific capacitance can be almost fully maintained after 2000 cycles at 1 A/g, and the shape of Nyquist plots is also well maintained (Figure 3f).

The excellent electrochemical properties of the aligned CNT/PANI composite electrode can be well maintained under both bending and stretching. The flexibility and

stretchability of the composite electrode had been first investigated by tracing the change of electrical resistances under bending and stretching (Figure 4a). Here the resistance was calculated from the voltage divided by current through a typical two-point measurement method. The resistance was fluctuated within 0.5% during bending for 1000 cycles (Figure S6). Figure S7a shows the dependence of the resistance on the strain during stretching, and it had been varied in less than 2.1% when the composite electrode was stretched to 100%. In addition, after the composite electrode had been stretched for 100 cycles at a strain of 100%, the resistance was slightly increased by 9.4% and then remained almost unchanged with the further increase to 200 cycles (Figure S7b). The crumpled composite electrode enabled a high flexibility and stretchability in the resulting device. The supercapacitors had been bent for over 1000 cycles and stretched for over 200 cycles without obvious fatigues in structure. Figure 4b further

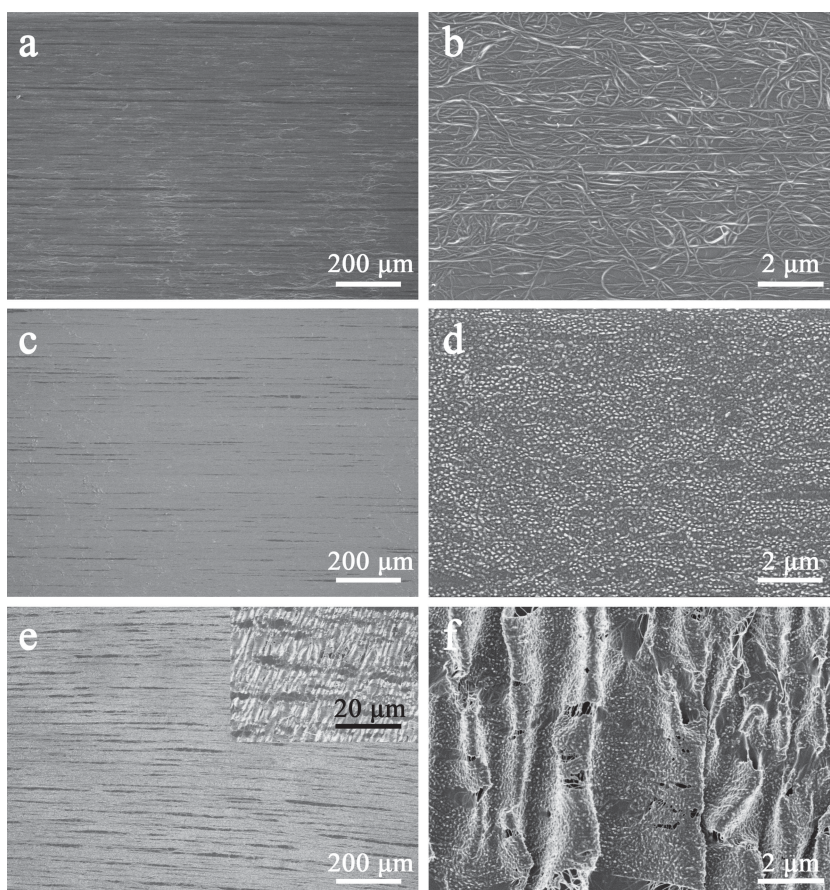


Figure 2. SEM images. a, b. Aligned CNT sheet on a stretched PDMS substrate at low and high magnifications, respectively. c, d. Aligned CNT/PANI composite on a stretched PDMS film at low and high magnifications, respectively. e, f. Aligned CNT/PANI composite on the released PDMS substrate at low and high magnifications, respectively. The inserted image is magnified from e.

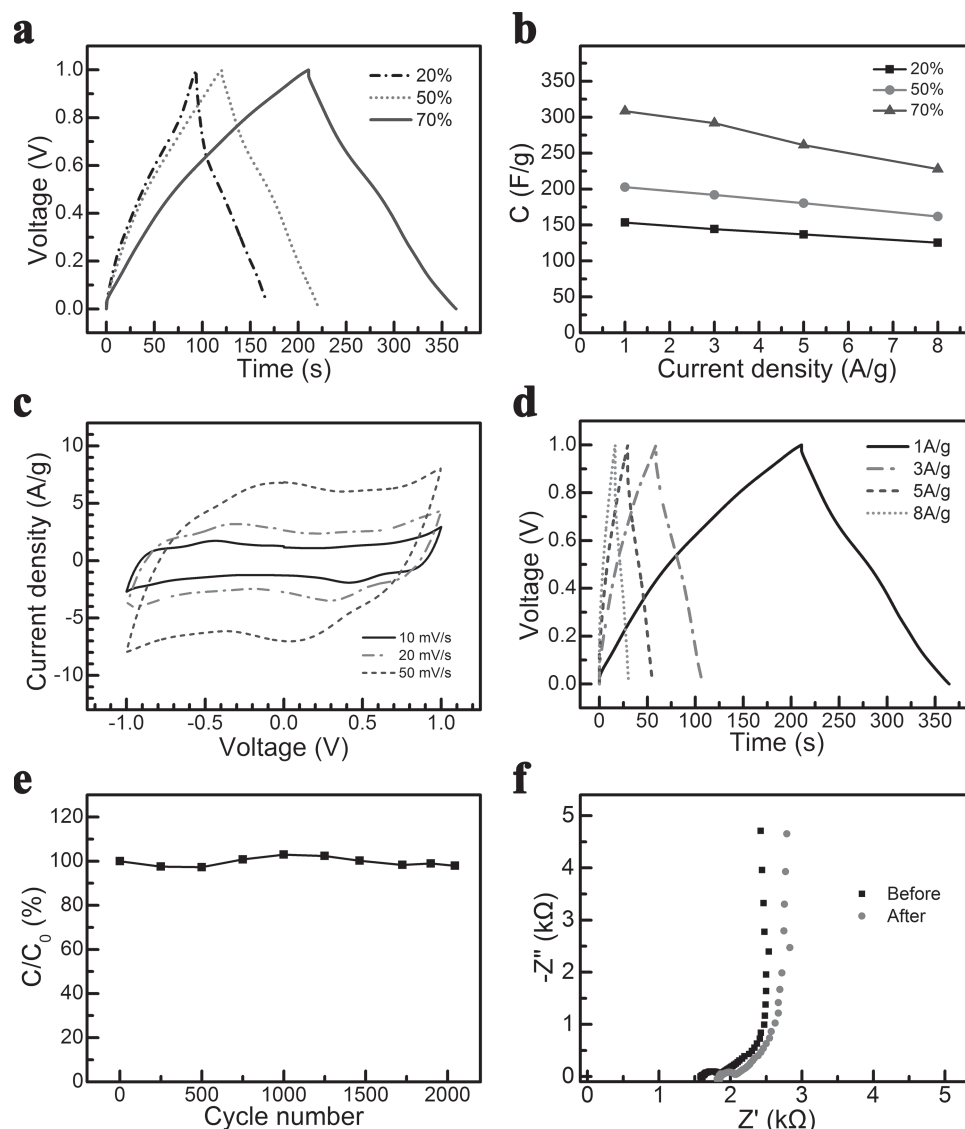


Figure 3. Electrochemical characterizations of the supercapacitor. a. Galvanostatic charge-discharge profiles of supercapacitors with different PANI weight percentages. b. Dependence of specific capacitance on PANI weight percentage and current density. c. Cyclic voltammograms with increasing scan rates. d. Galvanostatic charge-discharge profiles at increasing current densities. e. Dependence of specific capacitance on cycle number at a current density of 1 A/g. f. Nyquist plots before and after long-life cycles. The supercapacitor at c-f was fabricated based on the PANI weight percentage of 70% and the CNT thickness was 20 nm at a-f.

exhibits the specific capacitances at the bent and unbent states after 1000 cycles, and the capacitances had been well maintained by 95.8% in both cases. The capacitances were slightly increased by 1.9% and 1.8% when the supercapacitor was stretched by strains of 10% and 20%, respectively (Figure 4c). This phenomenon may be explained by the improved contact between the electrode and electrolyte induced by the shearing force during stretching. With the increasing strain to 30%, the capacitances were slightly decreased to 99.7% of the original value. With the further increase to 100%, the capacitances could be maintained by 80.8%. Upon release of the supercapacitor to the non-stretched state, the capacitance was 100% reverted to the original value. In particular, the capacitances

had been maintained by almost 100% after the supercapacitor was stretched for 200 cycles compared with the first stretched cycle (Figure 4d).

Interestingly, the supercapacitor exhibited different colors with the variation of voltages during the charging-discharging process (Figure 5). Upon the full charge with a voltage of 1 V, the positive electrode turned blue while negative electrode faded to yellow. When the supercapacitor was discharged to 0.5 V, the positive electrode changed to green while negative electrode remained yellow. With the further discharge to 0 V, both positive and negative electrodes turned light green. In contrast, the negative electrode became green while positive electrode turned yellow at -0.5 V; the negative electrode

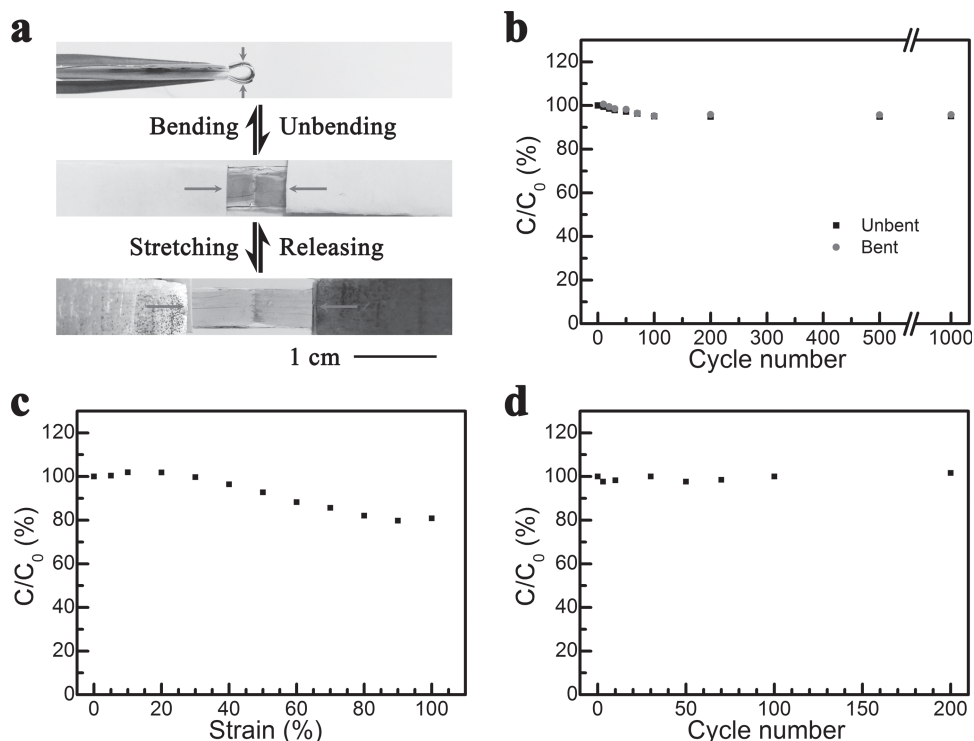
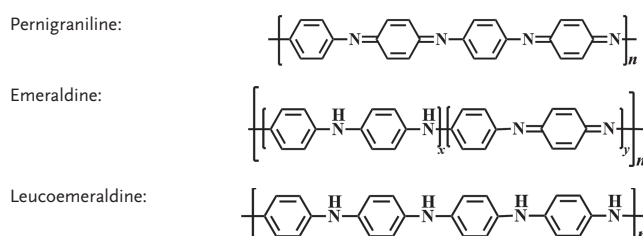


Figure 4. a. Photographs of a supercapacitor before and after bending and stretching. b. Dependence of specific capacitance on bent cycle number. c. Dependence of specific capacitance on strain. d. Dependence of specific capacitance on stretched cycle number at a strain of 100%. C_0 and C correspond to the specific capacitances before and after bending or stretching, respectively.

changed to blue while positive electrode remained yellow at -1 V, where the discharge process was completed. More details on the color changes are provided in Figure S8 and Video S1. The chromatic transitions were also reversible and could be directly caught by the naked eyes (Video S1). The chromatic transitions were further quantitatively characterized by UV-vis spectroscopy, and the positive electrode had been studied as a demonstration (Figure 5f). The characteristic absorbance peaks occurred at 669.4, 750, 793.8, 825.2 and 835.6 nm at the voltages of 1, 0.5, 0, -0.5 and -1 V, respectively. Note that although PANI has been widely explored as various sensing materials including electrochromatic nanocomposites,^[14b] to the best of our knowledge, this work represents the first demonstration on the realization of chromatic devices using PANI.

The mechanism for the chromatic transition in smart supercapacitor is summarized below. A positive electrode was investigated as a demonstration considering the symmetric structure in the supercapacitor. Conducting polymers have been shown to change structures under different oxidation states. Here PANI mainly demonstrate three structures below, i.e., leucoemeraldine that corresponds to a fully reduced state with amine linkers, pernigraniline that corresponds to a fully oxidized state with imine linkers and emeraldine that is composed of both amine and imine linkers. Here x and y correspond to the percentage of each format, while n represents the number of the repeating unit.



At 1 V, PANI appears blue at a pernigraniline form; at 0.5 V, it is partially reduced to the protonated emeraldine salt with a green color; at 0 V, it turns light green in a slightly oxidized state; at -0.5 and -1 V, it is fully reduced into a leucoemeraldine with a color change to yellow.^[28–31] Although the aligned CNT sheet mainly serves as a current collector, it was also found to greatly improve the electrochemical and thermal properties of the incorporated conducting polymers with high stability.^[13a,32] Therefore, a rapid and reversible transition had been achieved in the composite material. On the other hand, the aligned CNT/PANI composite formed a crumbled structure on the released PDMS substrate, which enabled a combined high stretchability, flexibility and electrochemical stability. Note that the stretchability of the smart supercapacitor was 100% as the used PDMS substrate showed a maximal stretchability of 100%. Based on the designed structure of the composite electrode, much higher stretchabilities can be achieved for the smart supercapacitor by using a PDMS with much higher strains. More efforts are

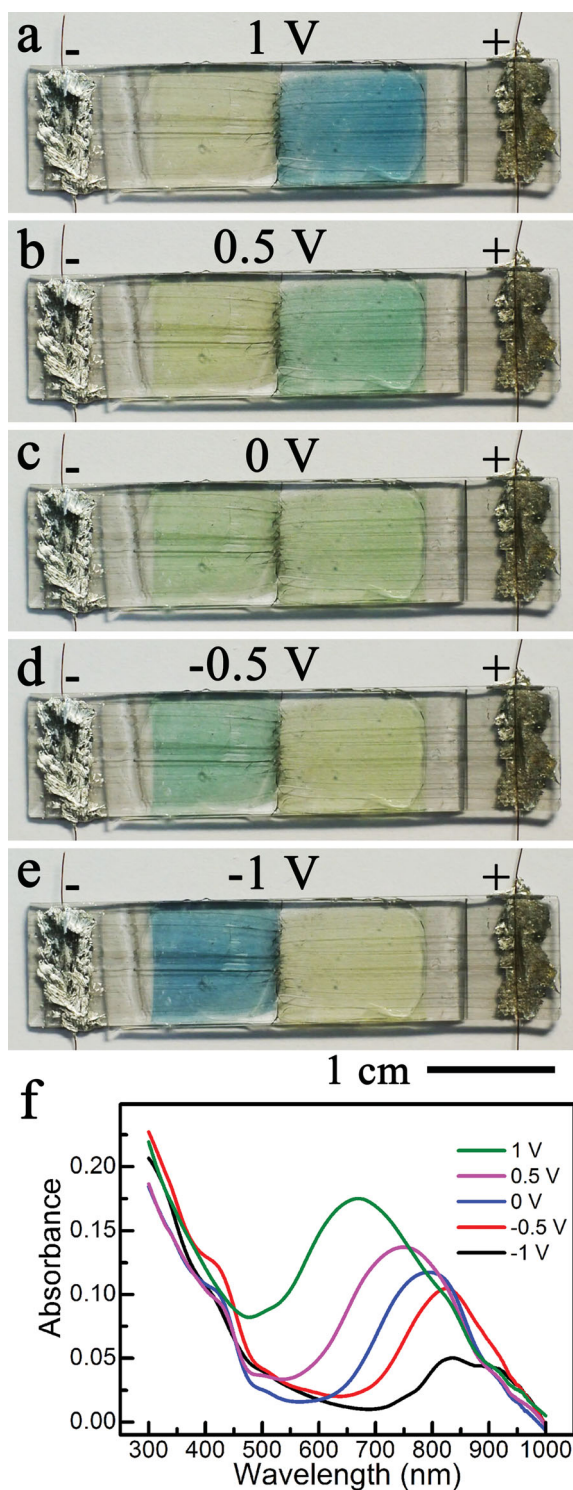


Figure 5. a-e. Chromatic transition during a charging-discharging process. f. UV-vis spectra of the positive electrode corresponding to the states at a-e.

underway to study new PDMS substrates with strains up to 800%.

In summary, a new family of smart, super-stretchy and flexible supercapacitors has been developed with high performances. The smart supercapacitors rapidly and reversibly

demonstrate color changes in a response to the variation on the level of stored energy. These supercapacitors also exhibit high specific capacitances that have been maintained by almost 100% after stretching at a strain of 100% for 200 cycles and 95.8% after bending for 1000 cycles. Although a conducting polymer has been mainly explored here, a wide variety of other electrochromatic materials such as metal oxide can be also used to make the smart supercapacitor. This work may serve as a starting point in designing smart supercapacitors to delivery new functionalities that remain challenging or even impossible to their conventional counterparts. Our design strategy can be also extended to the other energy conversion and storage devices besides supercapacitors.

Experimental Section

PDMS substrates with a thickness of 150 μm were fabricated by spin-coating a mixture of PDMS base/curing agent (Sylgard 184, Dow Chemical) with a mass ratio of 10/1 at 930 rpm for 10 s, followed by curing at 80 $^{\circ}\text{C}$ for 1 h. The aligned CNT sheet was dry-spun from spinnable CNT array synthesized according to the details described in the Supporting Information.^[18,33] PANI was electrodeposited onto aligned CNT sheets through an electropolymerization of aniline at a potential of 0.75 V in an aqueous solution of aniline (0.1 M) and H_2SO_4 (1 M) using KCl-saturated Ag/AgCl as a reference electrode and platinum wire as the counter electrode. The gel electrolyte was mixed from PVA aqueous solution and H_3PO_4 with the PVA/ H_3PO_4 mass ratio of 1/0.85, and the experimental details are described in the Supporting Information.^[34] The specific capacitances were calculated on the basis of the whole electrode.

Supporting Information

Supporting Information is available from the Wiley Online Library or from the author.

Acknowledgements

This work was supported by MOST (2011CB932503), NSFC (21225417), STCSM (12nm0503200), the Fok Ying Tong Education Foundation, the Program for Special Appointments of Professors at Shanghai Institutions of Higher Learning, Innovative Student Program at Fudan University (EZH2203302/002), and the Program for Outstanding Young Scholars from the Organization Department of the CPC Central Committee.

Received: February 25, 2014

Revised: March 23, 2014

Published online: May 2, 2014

- [1] Z. Wen, X. Wang, S. Mao, Z. Bo, H. Kim, S. Cui, G. Lu, X. Feng, J. Chen, *Adv. Mater.* **2012**, *24*, 5610–5616.
- [2] S. Li, D. Wu, C. Cheng, J. Wang, F. Zhang, Y. Su, X. Feng, *Angew. Chem. Int. Ed. Engl.* **2013**, *52*, 12105–12109.
- [3] Y. Huang, J. Liang, Y. Chen, *Small* **2012**, *8*, 1805–1834.
- [4] L. Zhang, X. Yang, F. Zhang, G. Long, T. Zhang, K. Leng, Y. Zhang, Y. Huang, Y. Ma, M. Zhang, Y. Chen, *J. Am. Chem. Soc.* **2013**, *135*, 5921–5929.
- [5] E. Iyyamperumal, S. Wang, L. Dai, *ACS Nano* **2012**, *6*, 5259–5265.

- [6] S. Mao, Z. Wen, H. Kim, G. Lu, P. Hurley, J. Chen, *ACS Nano* **2012**, *6*, 7505–7513.
- [7] D. Yu, L. Dai, *J. Phys. Chem. Lett.* **2010**, *1*, 467–470.
- [8] Z. S. Wu, Y. Sun, Y. Z. Tan, S. Yang, X. Feng, K. Mullen, *J. Am. Chem. Soc.* **2012**, *134*, 19532–19535.
- [9] Z. Cao, B. Wei, *Energy Environ. Sci.* **2013**, *6*, 3183–3201.
- [10] D. Wei, M. R. Scherer, C. Bower, P. Andrew, T. Ryhanen, U. Steiner, *Nano Lett.* **2012**, *12*, 1857–1862.
- [11] W. Qian, F. Sun, Y. Xu, L. Qiu, C. Liu, S. Wang, F. Yan, *Energy Environ. Sci.* **2014**, *7*, 379–386.
- [12] B. Qiu, C. Pan, W. Qian, Y. Peng, L. Qiu, F. Yan, *J. Mater. Chem. A* **2013**, *1*, 6373–6378.
- [13] a) H. Lin, L. Li, J. Ren, Z. Cai, L. Qiu, Z. Yang, H. Peng, *Sci. Rep.* **2013**, *3*, 1353; b) T. Chen, H. Peng, M. Durstock, L. Dai, *Sci. Rep.* **2014**, *4*, 3612; c) Z. Yang, J. Deng, X. Chen, J. Ren, H. Peng, *Angew. Chem. Int. Ed.* **2013**, *52*, 13453–13457
- [14] a) X. Sun, T. Chen, S. Huang, L. Li, H. Peng, *Chem. Soc. Rev.* **2010**, *39*, 4244–4257; b) H. Wei, X. Yan, S. Wu, Z. Luo, S. Wei, Z. Guo, *J. Phys. Chem. C* **2012**, *116*, 25052–25064.
- [15] a) H. Peng, X. Sun, F. Cai, X. Chen, Y. Zhu, G. Liao, D. Chen, Q. Li, Y. Lu, Y. Zhu, Q. Jia, *Nat. Nanotechnol.* **2009**, *4*, 738–741; b) X. Sun, Z. Zhang, X. Lu, G. Guan, H. Li, H. Peng, *Angew. Chem. Int. Ed.* **2013**, *52*, 7776–7780.
- [16] W. Wang, X. Sun, W. Wu, H. Peng, Y. Yu, *Angew. Chem. Int. Ed.* **2012**, *51*, 4644–4647.
- [17] Z. Yang, T. Chen, R. He, G. Guan, H. Li, L. Qiu, H. Peng, *Adv. Mater.* **2011**, *23*, 5436–5439.
- [18] H. Peng, *J. Am. Chem. Soc.* **2008**, *130*, 42–43.
- [19] J. Zang, S. Ryu, N. Pugno, Q. Wang, Q. Tu, M. J. Buehler, X. Zhao, *Nat. Mater.* **2013**, *12*, 321–325.
- [20] F. Huang, D. Chen, *Energy Environ. Sci.* **2012**, *5*, 5833–5841.
- [21] K. Wang, H. Wu, Y. Meng, Z. Wei, *Small* **2014**, *10*, 14–31.
- [22] K. Wang, J. Huang, Z. Wei, *J. Phys. Chem. C* **2010**, *114*, 8062–8067.
- [23] H. Zhang, G. Cao, Z. Wang, Y. Yang, Z. Shi, Z. Gu, *Electrochem. Commun.* **2008**, *10*, 1056–1059.
- [24] J. Yan, T. Wei, B. Shao, Z. Fan, W. Qian, M. Zhang, F. Wei, *Carbon* **2010**, *48*, 487–493.
- [25] Q. Wu, Y. Xu, Z. Yao, A. Liu, G. Shi, *ACS Nano* **2010**, *4*, 1963–1970.
- [26] D. Wei, H. Wang, P. Hiralal, P. Andrew, T. Ryhanen, Y. Hayashi, G. A. Amaratunga, *Nanotechnology* **2010**, *21*, 435702.
- [27] V. Gupta, N. Miura, *Electrochim. Acta* **2006**, *52*, 1721–1726.
- [28] T. Kobayashi, H. Yoneyama, H. Tamura, *J. Electroanal. Chem. Interf. Electrochem.* **1984**, *177*, 281–291.
- [29] A. A. Argun, P.-H. Aubert, B. C. Thompson, I. Schwendeman, C. L. Gaupp, J. Hwang, N. J. Pinto, D. B. Tanner, A. G. MacDiarmid, J. R. Reynolds, *Chem. Mater.* **2004**, *16*, 4401–4412.
- [30] R. J. Mortimer, *Electrochim. Acta* **1999**, *44*, 2971–2981.
- [31] D. M. DeLongchamp, P. T. Hammond, *Chem. Mater.* **2004**, *16*, 4799–4805.
- [32] Z. Cai, L. Li, J. Ren, L. Qiu, H. Lin, H. Peng, *J. Mater. Chem. A* **2013**, *1*, 258–261.
- [33] L. Qiu, X. Sun, Z. Yang, W. Guo, H. Peng, *Acta Chim. Sinica* **2012**, *70*, 1523–1532.
- [34] X. Chen, L. Qiu, J. Ren, G. Guan, H. Lin, Z. Zhang, P. Chen, Y. Wang, H. Peng, *Adv. Mater.* **2013**, *25*, 6436–6441.